Inorg. Chem. **2007**, *46*, 8403–8409

New Series of Indium Formates: Hydrothermal Synthesis, Structure and Coordination Modes

Jie Su, Yingxia Wang,* Sihai Yang, Guobao Li, Fuhui Liao, and Jianhua Lin*

Beijing National Laboratory for Molecular Sciences, State Key Laboratory of Rare Earth Materials Chemistry and Applications, College of Chemistry and Molecular Engineering, Peking University, Beijing 100871, P. R. of China

Received April 21, 2007

Three new indium(III) compounds, $In(HCOO)_3$ (**1**), $In_2(HCOO)_5(OH)$ (**2**), and $In(HCOO)_2(OH)$ (**3**), were synthesized under hydrothermal conditions and characterized by single crystal and powder X-ray diffraction experiments, as well as by IR spectroscopy, elemental analysis, and coupled TG-DSC–MS measurement. All of these compounds adopt 3D framework structures consisting of InO_6 octahedra and the 2.11 binding modes of formate with the (syn, syn-; syn, anti-; anti, anti-) configurations. The structural investigation of these indium formates reveals that the gradual introduction of the hydroxyl groups into the structures induces the polymerization of the InO_6 octahedra, that is, InO_6 is isolated in **1,** becomes dimeric in **2**, and finally forms 1D chains in **3**. In addition, a simple formula that may be used for estimating the overall coordination number of the formate in $M_a(HCOO)_bL_c$ is proposed.

Introduction

The versatility of carboxylate anions, as seen by their diverse coordination modes to metal centers, results in the formation of various new structural types for metal carboxylates. This has induced extensive studies on the syntheses, structures, and properties of these compounds.[1,2] Formate, as the simplest carboxylate with the smallest steric effect, has attracted considerable attention.[3−27] As a mono-, bis-, or polydentate ligand, formate can bind metal cations in various ways, as shown in Figure 1. The coordination mode

* To whom correspondence should be addressed: E-mail: jhlin@pku.edu.cn (J.L.), wangyx@pku.edu.cn (Y.W.). Fax: 86-10-62753541. Tel: 86-10-62751715, 86-10-62755538.

(1) Rao, C. N. R.; Natarajan, S.; Vaidhyanathan, R. *Angew. Chem., Int. Ed.* **2004**, *43*, 1466.
(2) Li, H. L.; Eddaoudi, M.; O'Keeffe, M.; Yaghi, O. M. *Nature* **1999**, *402*, 276.
(3) Sapiña, F.; Burgos, M.; Escrivá, E.; Folgado, J.; Marcos, D.; Beltrán, A.; Beltrán, D. *Inorg. Chem.* **1993**, *32*, 4337.
(4) Viertelhaus, M.; Anson, C. E.; Powell, A. K. *Z. Anorg. Allg. Chem.* **2005**, *631*, 2365.
(5) Viertelhaus, M.; Henke, H.; Anson, C. E.; Powell, A. K. *Eur. J. Inorg. Chem.* **2003**, 2283.
(6) Kageyama, H.; Khomskii, D. I.; Levitin, R. Z.; Vasil'ev, A. N. *Phys. Rev. B* **2003**, *67*, 224422.
(7) Radhakrishna, P.; Gillon, B.; Chevrier, G. *J. Phys.: Condens. Matter* **1993**, *5*, 6447.
(8) Nakayama, K.; Achiwa, N.; Fujino, M.; Matsugaki, N.; Yamagata, K. *J. Magn. Magn. Mater.* **1995**, *140*−*145*, 1745.
(9) Rettig, S. J.; Thompson, R. C.; Trotter, J.; Xia, S. *Inorg. Chem.* **1999**, *38*, 1360.
(10) Wang, X. Y.; Wei, H. Y.; Wang, Z. M.; Chen, Z. D.; Gao, S. *Inorg. Chem.* **2005**, *44*, 572.
(11) Wang, Y.; Cao, R.; Bi, W.; Li, X.; Yuan, D.; Sun, D. *Microporous Mesoporous Mater.* **2006**, *91*, 215.
(12) Dybtsev, D. N.; Chun, H.; Yoon, S. H.; Kim, D.; Kim, K. *J. Am. Chem. Soc.* **2004**, *126*, 32.
(13) Wang, Z. M.; Zhang, B.; Fujiwara, H.; Kobayashi, H.; Kurmoo, M. *Chem. Commun.* **2004**, 416.
(14) Wang, Z. M.; Zhang, B.; Kurmoo, M.; Green, M. A.; Fujiwara, H.; Otsuka, T.; Kobayashi, H. *Inorg. Chem.* **2005**, *44*, 1230.
(15) Cui, H. B.; Wang, Z. M.; Takahashi, K.; Okano, Y.; Kobayashi, H.; Kobayashi, A. *J. Am. Chem. Soc.* **2006**, *128*, 15074.
(16) Rood, J. A.; Noll, B. C.; Henderson, K. W. *Inorg. Chem.* **2006**, *45*, 5521.
(17) Viertelhaus, M.; Adler, P.; Clérac, R.; Anson, C. E.; Powell, A. K. *Eur. J. Inorg. Chem.* **2005**, 692.
(18) Wang, Z. M.; Zhang, B.; Otsuka, T.; Inoue, K.; Kobayashi, H.; Kurmoo, M. *J. Chem. Soc., Dalton Trans.* **2004**, 2209.
(19) Wang, X. Y.; Gan, L.; Zhang, S. W.; Gao, S. *Inorg. Chem.* **2004**, *43*, 4615.
(20) Wang, Z. M.; Zhang, B.; Inoue, K.; Fujiwara, H.; Otsuka, T.; Kobayashi, H.; Kurmoo, M. *Inorg. Chem.* **2007**, *46*, 437.
(21) Bolotovsky, R. L.; Bulkin, A. P.; Krutov, G. A.; Kudryashev, V. A.; Trunov, V. A.; Ul'yanov, V. A.; Antson, O.; Hiismäki, P.; Pöyry, H.; Tiitta, A.; Loshmanov, A. A.; Furmanova, N. G. *Solid State Commun.* **1990**, *76*, 1045.
(22) Ilyukhin, A. B.; Petrosyants, S. P. *Acta Cryst.* **2004**, *E60*, m151.
(23) Cornia, A.; Caneschi, A.; Dapporto, P.; Fabretti, A. C.; Gatteschi, D.; Malavasi, W.; Sangregorio, C.; Sessoli, R. *Angew. Chem., Int. Ed.* **1999**, *38*, 1780.
(24) Chaplygina, N. M.; Babievskaya, I. Z.; Kudinov, I. B. *Russ. J. Inorg. Chem.* (*Engl. Transl.*) **1984**, *29*, 1260.
(25) Chaplygina, N. M.; Babievskaya, I. Z.; Ivanov, N. I. *Russ. J. Inorg. Chem.* (*Engl. Transl.*) **1985**, *30*, 1218.
(26) Tian, Y. Q.; Zhao, Y. M.; Xu, H. J.; Chi, C. Y. *Inorg. Chem.* **2007**, *46*, 1612.
(27) Overgaard, J.; Rentschler, E.; Timco, G. A.; Larsen, F. K. *ChemPhysChem* **2004**, *5*, 1755.

10.1021/ic7007599 CCC: $37.00
Published on Web 08/29/2007

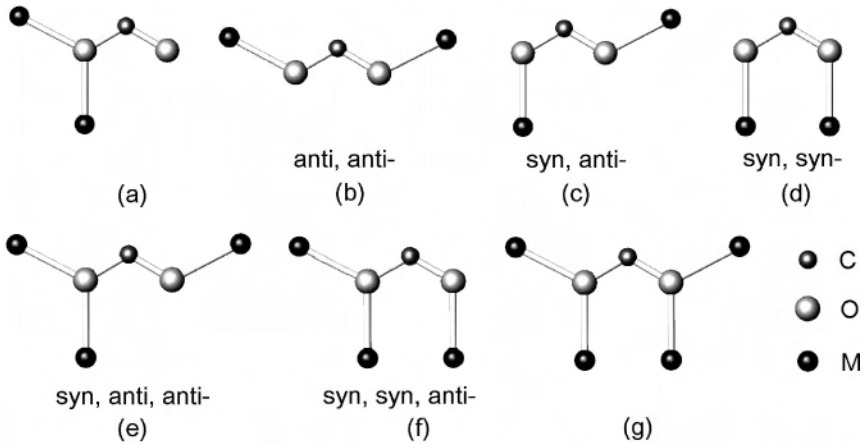

Figure 1. Possible coordination modes of formate ions.

of formates depends on the ratio of metal to formate and other co-ligands in the compounds. For example, in anhydrous divalent metal(II) formates $M(HCOO)_2$ (M = Fe, Co, Mn, Ni, Mg, Zn, Cu),[3−5] the coordination mode of the formate ions is μ_3 or, more precisely, a 3.21 bridging mode (by Harris notation[28]), whereas in their dihydrate forms $[M(HCOO)_2]\cdot 2H_2O$ (M = Fe, Co, Mn, Ni, Mg, Cu), the formate ions take μ_2 or a 2.11 binding mode, where the water molecules act as co-ligands to coordinate to the central atoms.[6−8] Other ligands, such as urea, formamide, 4,4′-bipyridine, etc., may also play a similar role to the water molecules.[8−11] Formates may also form microporous frameworks with enclosed guest molecules,[11−20] where the non-coordinated neutral molecules can be considered as ether templates or absorbed species,[12−17] and charged species, such as NH_4^+ and protonated amines, may not only act as templates but also can influence the connection mode of the formates by adjusting the ratio of metal to formate anion.[11,18−20]

The coordination mode of formate may also be influenced by the valence of central metal ions and their coordination preference. Trivalent metal formates are known[21−26] but are less extensively studied in comparison with the divalent metal formates. Rare earth formates, $Ln(HCOO)_3$ (Ln = Y, La, Ce, Tb, Tm), are typical examples for trivalent metal formates, in which the 9-coordinated rare earth ions are connected by the mode 3.21 of formate.[21] The structure of $Sc(HCOO)_3$, where scandium ions are octahedrally coordinated, presents an infinite 1D chain of ScO_6 octahedra connected by 2.11 (syn, syn-) formato bridges.[22] Furthermore, the trivalent metal formates, $[M(HCOO)_3]\cdot nG$ (M = Mn, Fe, Al, Ga, and In; G = guest molecules, such as CO_2, HCOOH, and absorbed H_2O),[23−26] adopt interesting porous frameworks related to the perovskite structure, in which the metal octahedra are bridged by formates in 2.11 (anti, anti) configuration. The diversity of the formate coordination modes is also exemplified by the structure of $Fe_2^{II}Fe_2^{III}(HCOO)_{10}(C_6H_7N)_6$, which is a mixed-valence compound consisting of neutral layers with 2.11 and 1.10 binding modes.[27] In this article, we report the synthesis and structures of three new indium(III) formates $In(HCOO)_3$ (**1**), $In_2(HCOO)_5(OH)$ (**2**), and $In(HCOO)_2(OH)$ (**3**). These compounds adopt 3D framework structures consisting of InO6 octahedra, which incorporate formate ions in three different bridging modes as shown by parts b−d of Figure 1. Additionally, the introduction of a hydroxyl group into the structures causes increasing polymerization of the InO_6 octahedra.

Experimental Section

Materials and Methods. The purity of the products was examined using powder X-ray diffraction on a Rigaku D/Max-2000 diffractometer with a Cu Kα radiation source (λ = 1.5418 Å) and a graphite monochromator at the secondary beam. Microinfrared spectroscopy was performed on a Nicolet Magna-IR 750 FTIR spectrophotometer in the region of 4000−650 cm^{-1}. Thermal analysis of the samples was done by a coupled TG−DSC−MS measurement using a NETZSCH STA 449C Jupiter/QMS. The MS measurement was taken for the volatile species from the decomposition of samples in an argon atmosphere with a heating rate of 10 °C/min from 25 to 400 °C, and prior to the measurement, the samples were evacuated at room temperature. The elemental analysis of carbon and hydrogen was carried out with an Elementar Vario EL III microanalyzer. The second-harmonic generation (SHG) coefficients were measured by the Kurtz−Perry method on powder samples. The wavelength of the incident light was 1064 nm from a YAG:Nd^{3+} laser, and the corresponding frequency-doubled outputs (λ = 532 nm) were recorded using KDP as a reference.

The starting materials for the syntheses were all commercially available and were used as purchased without further purification. The synthesis procedures of the compounds are described as follows.

$In(HCOO)_3$ (1). In_2O_3 (1 mmol, 0.2776 g), $HCOONa\cdot 2H_2O$ (6 mmol, 0.6242 g), and HCOOH (0.16 mol, 6 mL) were mixed in a 25 mL Teflon-lined stainless autoclave. The reaction was proceeded at 155 °C for 5 days. After cooling to room temperature, the solid was washed with formic acid, ethanol, and anhydrous diethyl ether, and then transparent club-shaped crystals were obtained. Anal. Calcd for $InC_3H_3O_6$ (fw 249.87): C 14.42, H 1.21. Found: C 14.29, H 1.35. An IR spectrum showed peaks (cm^{-1}, the intensity character is indicated following the position) at 2916w, 1635s, 1582vs, 1561s, 1402m, 1389s, 1374s, and 795m.

(28) Coxall, R. A.; Harris, S. G.; Henderson, D. K.; Parsons, S.; Tasker, P. A.; Winpenny, R. E. P. *J. Chem. Soc., Dalton Trans.* **2000**, 2349. (According to Harris notation, the binding mode is referred to as $[X.Y_1Y_2Y_3...Y_n]$, where the number before the decimal is the overall number of metals bound to the whole ligand, and each value of Y after the decimal represents the metal numbers attached to the different donor atoms.)

Table 1. Crystallographic Data and Structure Refinement Results for **1**−**3**

	1	**2**	**3**
chemical formula	$In(HCOO)_3$	$In_2(HCOO)_5(OH)$	$In(HCOO)_2(OH)$
fw	249.87	471.74	221.86
T (K)	298(2)	298(2)	298(2)
cryst syst	hexagonal	monoclinic	tetragonal
space group	$P6_3$	$P2_1/n$	$I\text{-}42d$
a (Å)	12.5464(18)	8.5742(17)	12.4199(4)
b (Å)	12.5464(18)	10.785(2)	12.4199(4)
c (Å)	6.9282(14)	12.445(3)	6.0842(3)
α (deg)	90	90	90
β (deg)	90	105.72(3)	90
γ (deg)	120	90	90
V (Å^3)	944.5(3)	1107.7(4)	938.51(6)
Z	6	4	8
D_c (g cm^{-3})	2.636	2.829	3.140
μ (Mo Kα) (mm^{-1})	3.724	4.217	4.959
cryst size (mm^3)	0.40 × 0.20 × 0.13	0.40 × 0.25 × 0.20	0.50 × 0.30 × 0.28
θ range (deg)	3.25−25.52	3.40−27.48	3.73−27.48
no. total reflns	1384	20 788	9140
no. unique reflns	650	2525	537
no. of obsd. reflns	646	1893	476
R_{int}	0.0301	0.0707	0.1111
R1, wR2 [$I > 2\sigma(I)$]	0.0158, 0.0368	0.0281, 0.0523	0.0244, 0.0465
R1, wR2 (all data)	0.0160, 0.0369	0.0494, 0.0557	0.0330, 0.0477
GOF	1.000	0.931	1.024

$In_2(HCOO)_5(OH)$ (2). A mixture of fresh $In(OH)_3$ (2 mmol, 0.3317 g, from indium chloride reacting with ammonia solution) and formic acid (0.16 mol, 6 mL) was placed in a 25 mL Teflon-lined stainless autoclave. The autoclave was sealed and heated to 165 °C in an oven under autogenous pressure for 8 days and then cooled to room temperature. Colorless crystalline product was filtered, washed with ethanol, and anhydrous diethyl ether and then dried at ambient temperature. Rhombic transparent crystals were obtained. Anal. Calcd for $In_2C_5H_6O_{11}$ (fw 471.74): C 12.72, H 1.28. Found: C 12.12, H 1.46. IR spectrum (cm^{-1}): 3492m, 2886w, 2864w, 2747w, 1620s, 1582vs, 1558s, 1533s, 1386s, 1370s, 970m, 810m, 802m, 759w, and 752w.

$In(HCOO)_2(OH)$ (3). $In(HCOO)_2(OH)$ was synthesized using fresh $In(OH)_3$ (2 mmol, 0.3317 g) and formic acid (0.16 mol, 6 mL) as starting materials. The reaction proceeded in a 25 mL Teflon-lined stainless autoclave at 175 °C in an oven for 5 days. The solid was washed with ethanol and anhydrous diethyl ether, and then transparent octahedral crystals were obtained. Anal. Calcd for $InC_2H_3O_5$ (fw 221.86): C 10.83, H 1.37. Found: C 10.78, H 1.62. IR spectrum (cm^{-1}): 3421m, 2918w, 2747w, 1609s, 1558vs, 1388m, 1359s, 1043m, 807w, 801w.

Crystallographic Studies. X-ray single-crystal diffraction data of **1** was collected on a Rigaku AFC6S diffractometer with graphite-monochromated Mo Kα radiation (λ = 0.71073 Å) by using the ω-2θ scan method at room temperature. The data of **2** and **3** were collected on a NONIUS Kappa-CCD with Mo Kα radiation (λ = 0.71073 Å) at 298 K. All of the structures were solved by the direct method and refined on F^2 with full-matrix least-squares methods using the *SHELXS-97* and *SHELXL-97* programs, respectively.[29] All of the non-hydrogen atoms were refined anisotropically. Hydrogen atoms were added in the riding model and refined isotropically with O−H = 0.94 Å and C−H = 0.93 Å. Crystallographic data and structure refinement results are summarized in Table 1. The corresponding CIF files are supplied in the Supporting Information.

(29) (a) Sheldrick, G. M. *SHELXS97, Program for Crystal Structure Solution*; University of Göttingen: Göttingen, Germany, 1997. (b) Sheldrick, G. M. *SHELXL97, Program for Crystal Structure Refinement*, University of Göttingen: Göttingen, Germany, 1997.

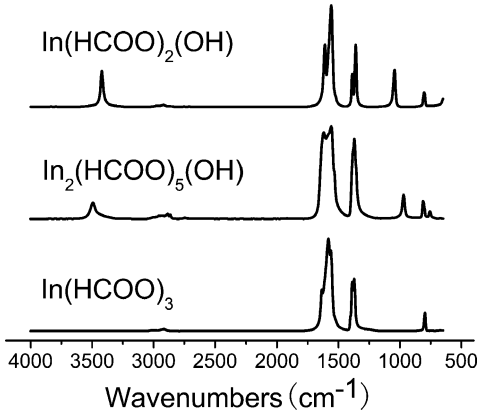

Figure 2. IR spectra of **1**−**3**.

Results and Discussion

Synthesis. The three compounds were synthesized in hydrothermal conditions. It has been found that the products are sensitive to the reaction conditions, especially to the starting materials and temperature (the bulk purities of the compounds were identified by powder X-ray diffraction (XRD) as shown in Figure S1 in the Supporting Information). At the beginning, formic acid (88%, wt/wt) was used to react with In_2O_3 in a sealed system in the temperature range of 50 to 160 °C; the product was always a mixture of **1** and residual In_2O_3, even though the reaction time was extended to 14 days. By adding a certain amount of $HCOONa{\cdot}2H_2O$ into the reaction system, pure $In(HCOO)_3$ sample, suitable for single-crystal diffraction analysis, was obtained. It is well-known that adding $HCOONa{\cdot}2H_2O$ into the formic acid solution increases the concentration of $HCOO^-$ and then suppresses the ionization degree of formic acid. Such $HCOOH/HCOO^-$ buffer solution is suitable for the formation of $In(HCOO)_3$. The reactions with more $HCOONa{\cdot}2H_2O$ were also examined, which resulted in the formation of a double-salt $Na_3In(HCOO)_6$. If the amount of $HCOONa{\cdot}2H_2O$ exceeded a certain value, In_2O_3 is unable to react with formic acid because of the low acidity.

2 and **3** were synthesized using the same starting materials, but at different temperatures. **2** forms at 165 °C, whereas **3** forms at 175 °C. These two products are both hydroxyformates with different OH^- to $HCOO^-$ ratios. In fact, both OH^- and $HCOO^-$ can coordinate to In^{3+} ions in the reaction system, and higher temperature seems to favor the formation of hydroxyl-endowed compounds. When the reaction temperature was higher than 180 °C, the product was always $In(OH)_3$, even though the starting materials were In_2O_3 and formic acid. A similar phenomenon was observed in the reaction of aluminum salts and formic acid. $Al(HCOO)_3{\cdot}HCOOH$ formed at 25−50 °C and hydrolyzed to $Al(HCOO)_2(OH)$ above 80 °C.[24,25]

IR Spectra and Thermal Properties. Figure 2 shows the IR spectra of the three compounds. The absorption bands at ∼1600, ∼1400, and ∼800 cm^{-1} correspond to the characteristic asymmetric stretching, symmetric stretching, and deformation vibrations of carboxyl groups COO^-, respectively. The typical vibrations of OH groups in **2** and

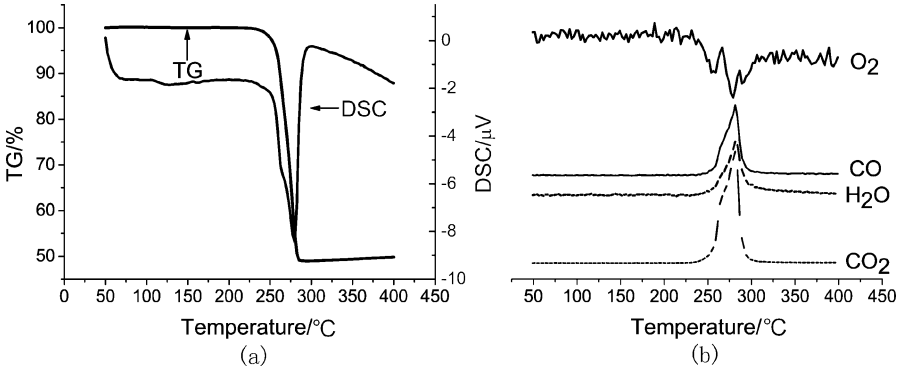

Figure 3. Coupled TG-DSC−MS analysis of **1**: (a) TG-DSC curve and (b) MS curve.

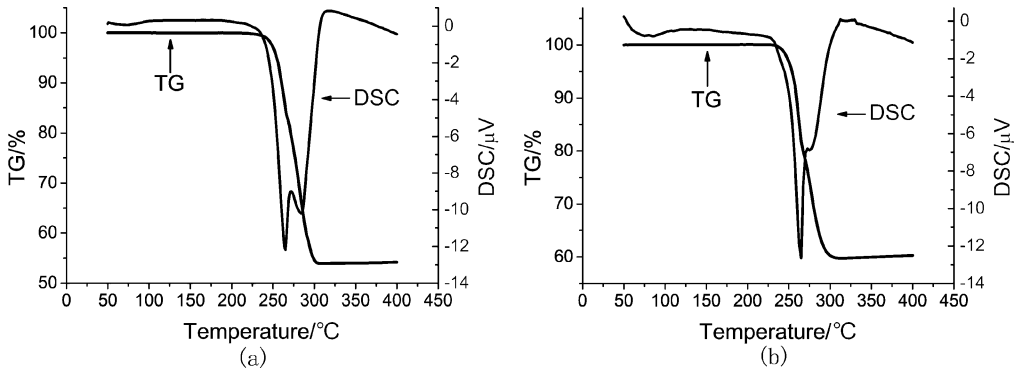

Figure 4. TG-DSC curves of (a) **2** and (b) **3**.

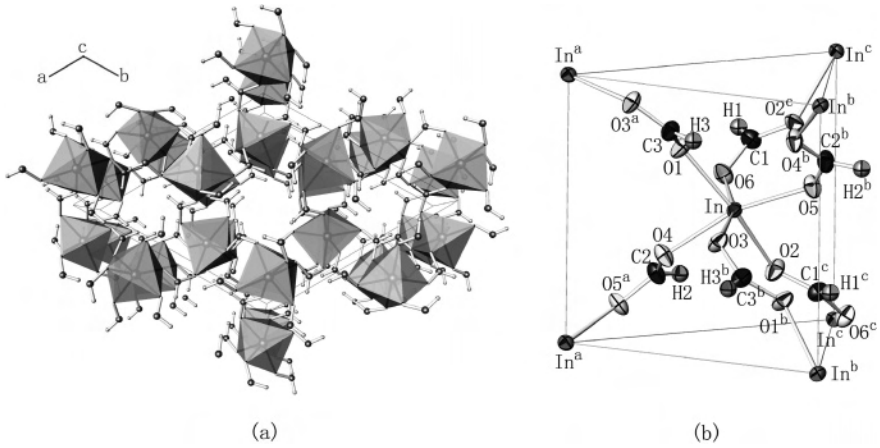

Figure 5. Structure of **1**: (a) View along the *c* axis, and (b) the connectivity of indium ions through formato bridges.

3 are present at 3400−3500 (stretching) and ∼1000 cm^{-1} (bending), respectively.

The thermogravimetric analysis results of the compounds under an argon atmosphere are shown in Figures 3 and 4. Similar thermal behavior was observed. **1** shows a weight loss at about 230−280 °C with an endothermal effect (Figure 3). The measured weight loss is about 50.60 wt %, which is significantly larger than the calculated value (44.44 wt %) based on the decomposition of $In(HCOO)_3$ to In_2O_3. For **2** and **3**, the thermal decomposition seems to take place in two steps, as indicated by the splitting of DSC peaks and a small slope change in the TG curves at about 250 °C (Figure 4). The measured total weight loss is about 46.01 wt % (Calcd 41.14 wt %) at 230−280 °C for **2** and 40.37 wt % (Calcd 37.42 wt %) at 230−300 °C for **3**, which are also higher than the expected values. To identify the decomposition products, **1**, **2**, and **3** were heated to 400 °C at a rate of 10 °C/min and then cooled to room temperature in a tube furnace under an argon atmosphere. The powder XRD profiles indicate that the decomposition products contain metal indium and In_2O_3 (Figure S2 in the Supporting Information). Obviously, the reduction of In_2O_3 occurs during the decomposition process. Because the decomposition of formate may produce the reductive gas CO, one should not be surprised that In_2O_3 is partially reduced in situ to elementary indium. In addition, the XRD patterns also show that the ratio of indium to In_2O_3 decreases from **1** (almost pure indium) to **3**, which is well consistent with the weight-loss data and may attribute to the decrease of the CO partial pressure from

Table 2. C−O Bond Distances (Angstroms) in **1**−**3**

$In(HCOO)_3$ (**1**)		$In_2(HCOO)_5(OH)$ (**2**)		$In(HCOO)_2(OH)$ (**3**)	
C3−O1	1.253(5)	C5−O1	1.246(5)	C1−O2	1.227(7)
C1−O2	1.237(5)	C2−O2	1.245(5)	C1−O3	1.258(6)
C3−O3	1.247(5)	C1−O4	1.251(5)		
C2−O4	1.243(5)	C1−O5	1.257(5)		
C2−O5	1.260(5)	C4−O6	1.235(5)		
C1−O6	1.249(5)	C4−O7	1.223(5)		
		C5−O8	1.224(5)		
		C3−O9	1.239(5)		
		C2−O10	1.250(5)		
		C3−O11	1.247(5)		

$In(HCOO)_3$ (**1**) to more OH-substituted $In(HCOO)_2(OH)$ **(3)** in the reaction system.

The MS result during the thermal decomposition of **1** is shown in part b of Figure 3. The observed species with the *m*/*z* values of 18, 28, and 44 can be assigned to H_2O, CO, and CO_2, respectively. These species show strong flux signals in the MS spectrum when the decomposition reaction takes place. The curve of $m/z = 32$ corresponds to O_2 (the data were multiplied by ∼25) that exists as a tiny impurity in the argon carrier gas. At the stage of formate decomposition, O_2 may be exhausted by CO and show depressed peaks.

Crystal Structure. In general, the structures of **1**, **2**, and **3** all consist of InO_6 octahedra and 2.11 formate bridges. However, the introduction of hydroxyl groups into the structures varies the formate/metal ratio, which induces the polymerization of the metal polyhedra.

$In(HCOO)_3$ (1). Part a of Figure 5 shows the structure of **1** projected along the *c* axis. The structure does contain channels, but they are too small (3×3 Å) to host guest molecules. The asymmetric unit of **1** contains 10 independent non-hydrogen atoms (1 indium, 3 carbons, and 6 oxygens) and three hydrogen atoms (part b of Figure 5). The indium atom is located in a distorted octahedron of oxygen atoms from formate ions with In−O bond distances in the range of 2.123 to 2.180 Å and O−In−O angles from 81.52 to 107.60°. The InO_6 octahedra are interconnected by six bridging formates in a centered trigonal prismatic network (part b of Figure 5). Each formate anion connects to two indium atoms in a 2.11 (syn, anti) mode. All of the C−O bond lengths fall into the range between the single C−O bond length (∼1.34 Å) and the double C−O bond length (∼1.21 Å), as listed in Table 2. The asymmetric parameter Δ [$\Delta = d$(C−O)-d(C−O′)] is very small in each formate group, which reflects the resonance effect of O−C−O in the formate group. **1** crystallizes in a noncentrosymmetric space group ($P6_3$). Thus, one would expect a nonlinear optical (NLO) effect. The NLO measurement was performed on powder samples using KDP as a reference, and the measured double-frequency output ($\lambda = 532$ nm) of this compound is 0.1 times of that of KDP, which also confirms the noncentrosymmetric structure of **1**.

$In_2(HCOO)_5(OH)$ (2). **2** crystallizes in the monoclinic space group $P2_1/n$. The structure contains 2 indium, 5 carbon, 11 oxygen, and 6 hydrogen independent sites. As far as the composition is concerned, **2** can be considered as a hydroxyl partly substituted derivative of **1**, in which one-sixth of the formate groups are replaced by hydroxyl groups. A consequence of the OH substitution is the dimerization of the InO_6 octahedra. As shown in part a of Figure 6, two InO_6 octahedra share a common hydroxyl group (μ_2-OH) to form an In_2O_{11} dimer. The InO_6 octahedra are all distorted, with the O−In−O angles in the range of 81.73 to 100.91° and In−O bond distances in the range of 2.090 to 2.179 Å. The bridging modes of formate in the structure of **2** are all the 2.11 bridges but with different configurations. In fact, all of the possible configurations of the 2.11 modes shown in parts b−d of Figure 1, that is, (anti, anti), (syn, anti), and (syn, syn) are present in the structure. The formates that bridge the octahedra within the dimer are in the (syn, syn) configuration, which leads to a 3-membered ring unit (2In + C). Such two dimers are connected by (anti, anti) formato bridges, forming a tetramer cluster as shown in part b of Figure 6, which are further linked through (syn, anti) formato bridges, forming a 3D structure. As shown in Table 2, the C−O bond lengths of the formate groups in the structure of **2** are in the range of 1.223−1.257 Å, which are similar to **1**, and well defined as the resonance effect of the formate groups. Consequently, the asymmetric parameter Δ of the formate group is also very small (0.022 Å).

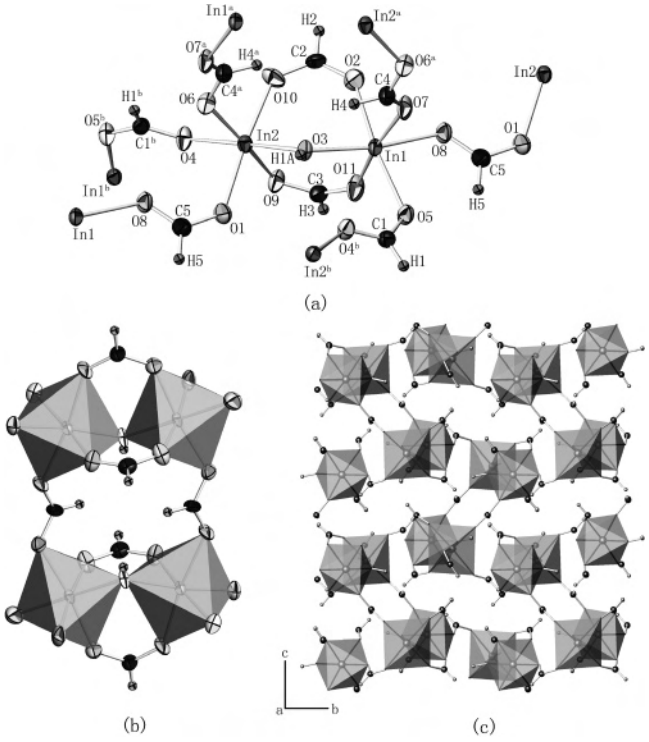

Figure 6. Coordination environment and formato bridge connections in the structure of **2**. (a) The dimer of InO_6 linked by the μ-OH group and (syn, syn) formato bridges. (b) The tetramer cluster formed by (anti, anti) formato-bridging dimers. (c) Projection along the *a* axis, showing (syn, anti) formato bridges between the tetramers.

$In(HCOO)_2(OH)$ (3). **3** could be considered as a further OH-substitution derivative of **2**, in which one-third of the formates are replaced by hydroxyl groups. The symmetry of the structure of **3** is quite high (*I*-42*d*) so that there are only 1 indium, 1 carbon, 2 oxygen, and 2 hydrogen sites in an asymmetric unit in the structure (part a of Figure 7). The indium ion is octahedrally coordinated by six oxygen atoms, four from formates, and two from hydroxyl groups. Similar

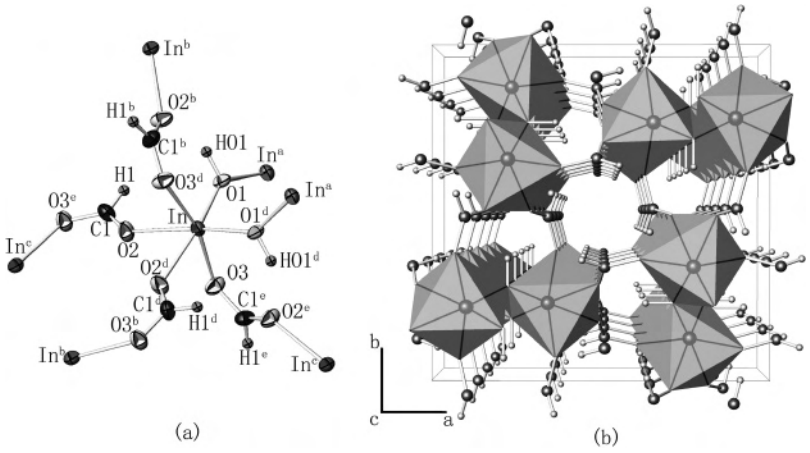

Figure 7. The structure of **3**: (a) the coordination environment of the indium atom and (b) viewed along the *c* axis.

to the other two compounds (**1** and **2**), the InO_6 octahedron is distorted, with the O−In−O angles in the range 74.2−103.51° and the In−O bond distances of 2.0991 Å (for the hydroxyl groups) and in the range of 2.173 to 2.199 Å (for the formates). Each InO_6 octahedron shares two corners (OH groups), forming a zigzag chain along the 2_1-screw axis, as shown in Figure 7b. The zigzag chains are interconnected by the 2.11 formato bridge of the (syn, anti) configuration. A small 1D channel exists along the *c* axis, but it is too small to host any guest molecules. The asymmetric parameter Δ of the formate groups is also very small (about 0.03 Å) for this compound. It is worth noting that both **1** and **3** have chains along the $2_1(6_3)$-screw axis. The difference is that the structure of **3** contains a corner-sharing octahedral zigzag chain along the 2_1-screw axis, whereas in **1**, the InO_6 octahedra forming the chain are isolated and connected by (syn, anti) formato bridges.

Coordination Modes of the Formato Bridge. Let us consider the binding mode of formate ions in a more general way. For a formate with the formula $M_a(HCOO)_bL_c$, one can deduce a simple equation to estimate the overall coordination number of the formate ion:

$$CN_{HCOO} = \frac{a \times CN_M - c \times CN_L}{b} \qquad (1)$$

here, CN_{HCOO}, CN_M, and CN_L represent the coordination numbers of the formate ion, the metal ion, and the co-ligand L, respectively. When the chemical formula and the coordination number of the metal and the L ligand are known, one could estimate the overall coordination number of the formate using eq 1. Eq 1 does not provide information about the bridging configuration, but from the experience, formate seems to prefer more-uniform coordination modes, such as 2.11, 3.21, or 4.22, instead of 2.20, 3.30, 4.40, and 4.31. The symmetrical coordination modes might get an advantage in energy from the uniform charge distribution and are useful for structure extension.

In the alkaline metal formates, M(HCOO) (M = Na, K, Rb, Cs), the metal ion is 8-coordinated ($CN_M = 8$), so we could get $CN_{HCOO} = 8$, according to eq 1. The observed bridging mode of formate in these monoformates is 8.44,[30] which means that the oxygen atom of the formate also has a high coordination number (μ_4-oxygen). This is largely due to the ionic M−O bond between M^+ and formate. Li(HCOO) is totally different from the other alkaline metal formates. In this structure, lithium ions are tetrahedrally coordinated ($CN_M = 4$), and the observed binding mode of the formate is 4.22.[31]

Now, we consider the divalent metal formate $M(HCOO)_2$. Supposing that the metal ion is 6-coordinated ($CN_M = 6$), for example in the transition metal formates, the coordination number of a formate should be 3 according to eq 1. The two possible bridging modes of 3.21 should be (syn, syn, anti) and/or (syn, anti, anti) (Figure 1), which means that in the structure, one of the oxygen atoms is monocoordinate and the other is μ_2-oxygen. If other ligands are involved in formates, eq 1 also can be used to predict the coordination number of the formate when the coordination number of the co-ligands is known. Considering a hydrated formate, $Mn(HCOO)_2 \cdot 2H_2O$, in which the manganese ions are 6-coordinated ($CN_M = 6$) and the water molecules are monocoordinated ($CN_L = 1$), the coordination number of the formate is $CN_{HCOO} = (6\text{-}1 \times 2)/2 = 2$. The observed bridging mode of the formates in the structure of $Mn(HCOO)_2 \cdot 2H_2O$ is 2.11 with the (syn, anti) and (anti, anti) configurations. In $[AmineH^+][Mn(HCOO)_3^-]$, the $AmineH^+$ is a charge compensator rather than a ligand, so we could deduce $CN_{HCOO} = (6 \times 1)/3 = 2$. The formato bridges in this compound are all in 2.11 of the (anti, anti) configuration.

For the trivalent metal formates, $M(HCOO)_3$ or $M_a(HCOO)_bL_c$, the mode 2.11 is very common if the metal ions are 6-coordinated. The indium formates discovered in this work present a nice series for trivalent systems. In $In(HCOO)_3$, the bridging mode of the formate is 2.11 with the (syn, anti) configuration. In $In_2(HCOO)_5(OH)$, one can obtain $CN_{HCOO} = (6 \times 2\text{-}1 \times 2)/5 = 2$ based on eq 1; for $In(HCOO)_2(OH)$, $CN_{HCOO} = (6\text{-}1 \times 2)/2 = 2$. However, the coordination configurations of the formates are quite complicated, although the bridging modes are all 2.11. The

(30) Wilson, M. P.; Alcock, N. W.; Rodger, P. M. *Inorg. Chem.* **2006**, *45*, 4359.
(31) Kansikas, J.; Hermansson, K. *Acta Crystallogr.* **1989**, *C45*, 187.

scandium ions (Sc^{3+}) in $Sc(HCOO)_3$ are 6-coordinated, so we could easily know that the bridging mode is 2.11. In the structure of $Sc(HCOO)_3$, the ScO_6 octahedra are interconnected by the formates with the (syn, syn) configuration, thereby forming 1D chains that run parallel and are organized through the van der Waals interaction.[22] For the rare earth formates, $Ln(HCOO)_3$ (Ln = La, Ce, Tb, Y, and Tm), the metal ions (Ln^{3+}) are 9-coordinated. Thus, we get $CN_{HCOO} = {}^9/_3 = 3$. In the structure of rare earth formates, LnO_9 is a tri-capped triangle prism, and the bridging mode of the formates is 3.21.[21] The LnO_9 polyhedra are connected via μ_2-oxo formato bridges, forming face-sharing chains, which are further linked via formato bridges to form a 3D framework.

Conclusion

Indium formate $In(HCOO)_3$ (**1**) and hydroxyl-endowed formates, $In_2(HCOO)_5(OH)$ (**2**) and $In(HCOO)_2(OH)$ (**3**), have been synthesized under hydrothermal conditions by slightly changing the starting materials and the reaction temperatures. At higher temperatures, the OH-substituted formates formed. The introduction of hydroxyl groups into the structures induces the polymerization of the InO_6 octahedra. In the hexagonal structure **1**, the InO_6 octahedra are isolated and bridged by the mode 2.11 of formate with the (syn, anti) configuration. In monoclinic structure **2**, the formates that connect InO_6 octahedra to the dimer In_2O_{11} are in the (syn, syn) configuration. Two dimers are bridged by (anti, anti) formato bridges, forming a tetramer cluster, which are further linked through (syn, anti) formato bridges to form a 3D structure. All three different coordination configurations of the 2.11 mode are present in **2**. In the tetragonal structure **3**, the InO_6 octahedra form 1D chains through sharing corners with μ_2-OH groups, which are further interconnected by the 2.11 (syn, anti) formates.

To illuminate the binding modes of formates, we proposed an equation for estimating the coordination number of the formate ions in $M_a(HCOO)_bL_c$. This is a simple way that can be applied not only to **1**−**3** but also to the other formates found in the literature.

Acknowledgment. The authors thank Prof. Zheming Wang for single-crystal data collection and helpful discussion on structural details. This study is financially supported by National Natural Science Foundation of China (Grants NSFC 20571004 and 20531010).

Supporting Information Available: Crystallographic data in CIF format for **1**−**3**. Powder XRD profiles of compounds $In(HCOO)_3$ (**1**), $In_2(HCOO)_5(OH)$ (**2**), $In(HCOO)_2(OH)$ (**3**), and their corresponding decomposition products. This material is available free of charge via the Internet at http://pubs.acs.org.

IC7007599